PHYSICAL REVIEW LETTERS **132,** 146801 (2024)

Macroscopic Polarization from Nonlinear Gradient Couplings

Massimiliano Stengel[*]
Institut de Ciència de Materials de Barcelona (ICMAB-CSIC), Campus UAB, 08193 Bellaterra, Spain
and ICREA–Institució Catalana de Recerca i Estudis Avançats, 08010 Barcelona, Spain

(Received 13 April 2023; accepted 14 February 2024; published 4 April 2024)

We show that a lattice mode of arbitrary symmetry induces a well-defined macroscopic polarization at first order in the momentum and second order in the amplitude. We identify a symmetric flexoelectric-like contribution, which is sensitive to both the electrical and mechanical boundary conditions, and an antisymmetric Dzialoshinskii-Moriya-like term, which is unaffected by either. We develop the first-principles methodology to compute the relevant coupling tensors in an arbitrary crystal, which we illustrate with the example of the antiferrodistortive order parameter in $SrTiO_3$.

DOI: 10.1103/PhysRevLett.132.146801

The interaction between structural, polar, and magnetic degrees of freedom in multiferroics has long been identified as a promising source of advanced material functionalities. The recent focus on inhomogeneous structures such as skyrmions [1], domain walls [2], and vortices [3,4] has renewed the interest in the so-called *Lifshitz invariants* (LIs), i.e., coupling terms that depend on the first gradient of one order parameter component. LIs play a key role in the stabilization of spatially modulated phases [5–7] and often determine their emerging physical properties. A paradigmatic example is the macroscopic Dzyaloshinskii-Moryia (DM) [8,9] interaction,

$$E_{\mathrm{DM}} = \zeta \mathbf{P}\cdot[\boldsymbol{\phi}(\boldsymbol{\nabla}\cdot\boldsymbol{\phi}) - (\boldsymbol{\phi}\cdot\boldsymbol{\nabla})\boldsymbol{\phi}], \tag{1}$$

where P is the macroscopic polarization, and $\boldsymbol{\phi}$ may correspond to the magnetic [10] or antiferromagnetic [11] degrees of freedom. [Realizations of Eq. (1) in other contexts, e.g., in liquid crystals [12] also exist.] The importance of Eq. (1) lies in its topological character [13], and the rich phenomenology it can lead to, ranging from the switchable P in ferroelectric multiferroics [10] to the stabilization of incommensurate spin orders in broken-symmetry environments.

Another category of LIs involves couplings between P and the gradients of a dyadic product $\phi_\gamma\phi_\lambda$,

$$E_{\mathrm{flexo}} = \frac{K_{\alpha\beta\gamma\lambda}}{2}\left[\frac{\partial P_\alpha}{\partial r_\beta}\phi_\gamma\phi_\lambda - P_\alpha\frac{\partial(\phi_\gamma\phi_\lambda)}{\partial r_\beta}\right]. \tag{2}$$

Equation (2) bears obvious similarities to flexoelectricity [14,15], where the symmetric strain tensor $\varepsilon_{\gamma\lambda}$ replaces the dyadic $\phi_\gamma\phi_\lambda$. Furthermore, as in the flexoelectric case the coupling tensor $K_{\alpha\beta\gamma\lambda}$ is a universal property of all crystals, hence its fundamental and practical interest. At difference with flexoelectricity, however, Eq. (2) describes a much broader class of *nonlinear* couplings, involving an arbitrary (pseudo)vector $\boldsymbol{\phi}$ [e.g., the ferroelectric polarization [16] or the antiferrodistortive (AFD) tilts [5] in perovskite-structure oxides] as main order parameter.

Research efforts are currently directed at exploring practical realizations of these ideas in a variety of materials and order parameter types [17]. It would be highly desirable, for instance, to find nonmagnetic analogues of Eq. (1), in contexts where the strength of the coupling constant ζ is not limited by weak relativistic effects [18]. The so-called ferroelectric DM interaction [18–20], which involves the polarization itself as the primary order parameter, appears as an especially promising candidate. An antiferrodistortive realization of Eq. (1) was also hinted at in Ref. [21], although the relationship between the "rotopolar" coupling described therein and Eq. (1) is not immediately obvious. Meanwhile, additional *indirect* contributions to P have also been pointed out, either involving the strain ("flexoroto" [22] effect in the case of tilts) or other nonpolar degrees of freedom (e.g., the antiferroelectric R mode of Refs. [21] and [23]). The coexistence of several effects, whose mutual relationship is sometimes paradoxical [5], complicates the understanding of flexo- and DM-type couplings, calling for a fundamental treatment.

The main priority for microscopic theory lies in clarifying the physical mechanisms that generate a polarization in inhomogeneous ferroic structures, either directly via Eqs. (1) and (2), or via the aforementioned indirect routes. In particular, it is of central importance to know whether these effects are well-defined bulk properties of the crystal, or whether they are plagued by ambiguities (e.g., due to boundary issues) as in the case of flexoelectricity [24,25]. At the same time, it would be desirable to establish an efficient and accurate methodological framework to predict the value of the relevant coupling coefficients in real materials, e.g., via first-principles techniques. Selected components of the rotopolar tensor in $SrTiO_3$ have been calculated already [21]; however, conceptual and technical difficulties with the treatment of spatial dispersion effects at nonlinear order have so far thwarted the development of a full-fledged theory.

Here, we provide a unified first-principles theory of both flexo- and DM-type couplings by expressing them as, respectively, the symmetric and antisymmetric parts of the same fourth-rank tensor. Based on this result, we argue that an arbitrary inhomogeneous field $\boldsymbol{\phi}$ always couples to polar degrees of freedom via both mechanisms, with the special case where $\mathbf{P}$ and $\boldsymbol{\phi}$ are the *same* mode as an interesting exception. We further show that the DM-like coefficient ζ is a well-defined physical property of the crystal, while the flexo-type tensor, $K_{\alpha\beta\gamma\lambda}$, is not. The reason lies in the macroscopic elastic and electrostatic interactions, which contribute to the latter but not to the former. Similarly to the flexoelectric case, these long-ranged ("nonanalytic," in the language of perturbation theory) terms lead to ambiguities in the definition of the reference electrostatic potential and the center of mass of the cell [24,25], which must be adequately treated to guarantee the internal consistency of the theory [26]. From a practical point of view we recast the nonlinear interaction between modulated order parameters as well-defined third derivatives of the total energy. The long-wavelength expansion [25,27] of the latter, which we treat in the framework of density-functional perturbation theory [28,29] (DFPT), readily yields the coupling constants of Eqs. (2) and (1) at first order in the momentum. Calculations are performed with minimal effort via the recently developed [25,27] long-wave module of ABINIT [30,31], in combination with a postprocessing tool that we have implemented and tested as part of this work [32]. As a numerical demonstration, we focus on the leading terms involving the AFD order parameter in $\mathrm{SrTiO_3}$.

Following Ref. [21], we base our derivations on *unsymmetrized* inhomogeneous couplings of the type

$$E_{\mathrm{uns}} = -W_{\alpha\beta\gamma\lambda} p_\alpha \frac{\partial \phi_\gamma}{\partial r_\beta} \phi_\lambda, \tag{3}$$

where E_{uns} is an energy per unit cell, $\boldsymbol{\phi}(\mathbf{r})$ is the main order parameter, and the field $\mathbf{p}(\mathbf{r})$ corresponds to some polar lattice mode of the crystal. Equation (3) is the most general trilinear coupling between $\boldsymbol{\phi}(\mathbf{r})$ and $\mathbf{p}(\mathbf{r})$ occurring at first order in the gradient expansion; any other expression can be written as a linear combination thereof. To verify this point explicitly in the case of Eqs. (2) and (1), it suffices to separate the symmetric and antisymmetric contributions with respect to the last two indices, $W_{\alpha\beta\gamma\lambda} = W_{\alpha\beta(\gamma\lambda)} + W_{\alpha\beta[\gamma\lambda]}$. Within the assumed cubic symmetry, elementary calculus leads then to

$$W_{\alpha\beta\gamma\lambda} = \underbrace{2K_{\alpha\beta\gamma\lambda}}_{W_{\alpha\beta(\gamma\lambda)}} + \underbrace{\zeta(\delta_{\alpha\gamma}\delta_{\beta\lambda} - \delta_{\alpha\lambda}\delta_{\beta\gamma})}_{W_{\alpha\beta[\gamma\lambda]}}, \tag{4}$$

which establishes the formal link between Eq. (3) and Eqs. (2) and (1). In a cubic crystal, $\mathbf{K}$ has three independent entries ($K_{11} = K_{1111}$, $K_{12} = K_{1122}$, and $K_{44} = K_{1212}$), similarly to the flexoelectric tensor. These, in combination with the DM-type scalar ζ, account for the four components of the tensor $\mathbf{W}$; the latter coincides with the rotopolar coupling of Ref. [21] in the AFD case.

The special case where $\boldsymbol{\phi} = \mathbf{p}$, of relevance to the recently proposed "electric DM interaction" [18,20], deserves a separate discussion. Equation (3) reduces then to Eq. (2) via a permutation of indices and integration by parts. This means that the DM-type coupling of Eq. (1) is redundant in this case: the flexo-type expression of Eq. (2) describes the trilinear self-interaction of a polar vector field in full generality. Assuming cubic symmetry of the undistorted crystal, Eq. (2) adopts the following compact form,

$$E_{\mathrm{p}} = K p^2 \boldsymbol{\nabla} \cdot \mathbf{p}, \tag{5}$$

where $K = K_{12} - K_{44}$ is a single material coefficient, and $p^2 = \mathbf{p} \cdot \mathbf{p}$. The remaining independent components of the $\mathbf{K}$ tensor (K_{11} and $K_{12} + K_{44}$) are irrelevant at the bulk level as they do not contribute to the forces nor to the energy. Crucially, Eq. (5) depends directly on the longitudinal components of $\mathbf{p}$, which are typically suppressed by depolarizing effects; for this reason, henceforth we shall restrict to our attention to cases where the primary order parameter $\boldsymbol{\phi}$ is nonpolar.

To work our way toward a first-principles expression, we need to specify the microscopic nature of the field variables entering Eq. (3). Following Ref. [26], we use a perturbative approach in terms of monochromatic lattice distortions of the type

$$u^l_{\kappa\alpha} = u^{\mathbf{q}}_{\kappa\alpha} e^{i\mathbf{q}\cdot\mathbf{R}^{(0)}_{l\kappa}}. \tag{6}$$

Here, κ and l are sublattice and cell indices, respectively; $u^l_{\kappa\alpha}$ indicates the atomic displacement along the Cartesian direction α; $\mathbf{R}^{(0)}_{l\kappa}$ stands for the unperturbed atomic locations in the high-symmetry reference structure; $\mathbf{q}$ is the momentum. The microscopic representation of the continuum fields is then defined as

$$u^{\mathbf{q}}_{\kappa\alpha} = \langle \kappa\alpha | p_\beta \rangle p^{\mathbf{q}}_\beta + \langle \kappa\alpha | \phi_\beta \rangle \phi^{\mathbf{q}}_\beta, \tag{7}$$

where the symbol $\langle \kappa\alpha | v \rangle$ corresponds [33] to the eigendisplacements of a given phonon mode $|v\rangle$, and $\mathbf{v}^{\mathbf{q}}$ refers to the Fourier representation of the field $\mathbf{v}(\mathbf{r})$. (Bra and kets refer to real vectors in the $3N$-dimensional space of the atomic displacements, where N is the number of basis atoms in the cell [33]).

Based on the above, we can express Eq. (3) in reciprocal space as a three-phonon vertex,

$$E_{\mathrm{uns}} = -iq_\beta W_{\alpha\beta\gamma\lambda} p_\alpha^{-\mathbf{q}-\mathbf{q}'} \phi_\gamma^{\mathbf{q}} \phi_\lambda^{\mathbf{q}'}. \tag{8}$$

In the $\mathbf{q}, \mathbf{q}' \to 0$ limit, we can then write the tensor $\mathbf{W}$ in terms of the third derivatives of the total energy E,

$$\frac{\partial^3 E}{\partial p_\alpha^{-\mathbf{q}} \partial \phi_\gamma^{\mathbf{q}} \partial \phi_\lambda^0} = \left\langle p_\alpha \middle| \frac{\partial \mathbf{\Phi}^{\mathbf{q}}}{\partial \phi_\lambda^0} \middle| \phi_\gamma \right\rangle, \tag{9}$$

or equivalently as the first derivative of the force-constant matrix $\mathbf{\Phi}^{\mathbf{q}}$ with respect to the homogeneous perturbation ϕ_λ^0. By recalling [24,25] the long-wave expansion of $\mathbf{\Phi}^{\mathbf{q}}$, $\mathbf{\Phi}^{\mathbf{q}} \simeq \Phi^{(0)} - iq_\beta \Phi^{(1,\beta)}$, we arrive then at a closed expression for the $\mathbf{W}$-tensor components as projection on the polar mode $\langle p_\alpha|$ of the *force-response tensor* $|w_{\beta\gamma\lambda}\rangle$,

$$W_{\alpha\beta\gamma\lambda} = \langle p_\alpha | w_{\beta\gamma\lambda} \rangle, \qquad |w_{\beta\gamma\lambda}\rangle = \frac{\partial \Phi^{(1,\beta)}}{\partial \phi_\lambda^0} |\phi_\gamma\rangle, \tag{10}$$

describing the forces $(\mathbf{f}_\kappa)$ on individual sublattices via $f_{\kappa\alpha} = \langle \kappa\alpha | w_{\beta\gamma\lambda} \rangle (\partial\phi_\gamma / \partial r_\beta) \phi_\lambda$. Thanks to cubic symmetry, Eq. (10) allows one to capture all the independent components of $\mathbf{W}$ at once as part of a single linear-response calculation; the flexo-like and DM-like contributions are then extracted via Eq. (4). Whenever appropriate, the mode index will be indicated with a superscript, either in the form $W^{(i)}_{\alpha\beta\gamma\lambda}$ or $W^{[i]}_{\alpha\beta\gamma\lambda}$ for the normal-mode or symmetry-adapted [34] sublattice representation [33] of the tensors, respectively.

Our next goal is to understand whether $\mathbf{W}$ (or its decomposition into $\mathbf{K}$ and ζ) is a well-defined physical property of the crystal. A first concern lies in the definition of the force-response tensor $|w_{\beta\gamma\delta}\rangle$, via a long-wave expansion of $\mathbf{\Phi}^{\mathbf{q}}$. To perform the latter operation, short-circuit electrical boundary conditions need to be imposed [24], which implies setting to zero the macroscopic electrostatic potential V^{mac} in the calculations. V^{mac} is, however, ill defined in a periodic crystal [35], which leads to a "reference potential ambiguity" in the definition of the flexo-type coefficients [24,25,36]. Note that this issue only affects the longitudinal components of the polarization. These are expected to be small in all but a few materials (e.g., hyperferroelectrics [37]) where depolarizing effects are unusually weak, so we will not delve into it further here. In any case, the DM-type constant ζ is manifestly unaffected by electrostatics, due to the transverse nature of Eq. (1).

A second issue concerns the translational freedom of the polar mode eigendisplacement vector, which is only defined modulo a rigid shift of the cell [26]. Based on the criteria of Ref. [26], a necessary condition for a material property to be "well defined" is its invariance with respect to the following transformation,

$$|p'_\alpha\rangle = |p_\alpha\rangle + \lambda, \tag{11}$$

where λ is an arbitrary constant. To understand the impact of Eq. (11) on $\mathbf{W}$, recall that the acoustic eigendisplacement vector reduces to a translation [26,36] regardless of the microscopics $\langle \kappa\alpha | u_\beta \rangle = \delta_{\alpha\beta}$. This implies that

$$W'_{\alpha\beta\gamma\delta} = W_{\alpha\beta\gamma\delta} + \lambda \langle u_\alpha | w_{\beta\gamma\delta} \rangle, \tag{12}$$

where $\langle u_\alpha | w_{\beta\gamma\delta} \rangle$ is a net elastic force on the cell as a whole that arises in a locally inhomogeneous order parameter $\boldsymbol{\phi}$. That such a force does not vanish is a direct consequence of the *strain coupling*

$$E_{\mathrm{sc}} = -R_{\alpha\beta\gamma\delta} \varepsilon_{\alpha\beta} \phi_\gamma \phi_\delta, \tag{13}$$

which is always allowed by symmetry. Since the force is the divergence of the stress, a trivial integration by parts leads to the following *sum rule*,

$$-\frac{1}{2} \sum_\kappa \langle \kappa\alpha | w_{\beta\gamma\lambda} \rangle = R_{\alpha\beta\gamma\lambda}, \tag{14}$$

relating the sublattice sum of the force-response tensor $|w_{\beta\gamma\lambda}\rangle$ to the strain coupling tensor $\mathbf{R}$. After observing that $R_{\alpha\beta\gamma\lambda}$ is symmetric both in $\alpha\beta$ and $\gamma\lambda$, we arrive at the following transformation law for the coupling coefficients,

$$K'_{\alpha\beta\gamma\delta} = K_{\alpha\beta\gamma\delta} - \lambda R_{\alpha\beta\gamma\delta}, \qquad \zeta' = \zeta. \tag{15}$$

Equation (15) is one of the central results of this work, showing that the DM-like coupling constant, unlike $\mathbf{K}$, is indeed invariant with respect to Eq. (11), and hence a well-defined bulk property, as anticipated earlier.

Notwithstanding the aforementioned ambiguity of $\mathbf{K}$, the information contained in it is crucial to obtaining a well-defined value of the local polarization at leading order in ϕ and $\mathbf{q}$. To see this, we assume in the following that the fields are modulated along a single direction $\hat{s}$ and constant along the normal planes. (This is appropriate, for example, to modeling a domain wall oriented along $\hat{s}$.) Within these mechanical boundary conditions, we obtain (see Supplemental Material, Sec. S8 [33]) the relaxed electrical polarization as (summation over repeated indices is implied)

$$P_\alpha = \frac{1}{\Omega} Z^{[i]} \Phi^{+}_{ij} \left(\tilde{K}^{[j]}_{\alpha\gamma\lambda}(\hat{s}) \mathcal{S}_{\gamma\lambda,s} + \zeta^{[j]} \mathcal{A}_\alpha \right), \tag{16}$$

where Φ^+ is the pseudoinverse [25,34,38] of the zone-center force-constants matrix; $\mathcal{S}_{\gamma\lambda,s} = \partial(\phi_\gamma \phi_\lambda)/\partial s$ and $\mathcal{A}_\alpha = \phi_s \partial\phi_\alpha/\partial s - \phi_\alpha \partial\phi_s/\partial s$ are the relevant symmetric and antisymmetric components of the nonlinear ϕ-gradient tensor; $Z^{[i]}$ are the mode dynamical charges; and the renormalized flexo-like coefficients are

$$\tilde{K}^{[j]}_{\alpha\gamma\lambda}(\hat{s}) = K^{[j]}_{\alpha\hat{s}\gamma\lambda} + C^{[j]}_{\alpha\hat{s}\beta\hat{s}} [\mathcal{C}(\hat{s})]^{-1}_{\beta\sigma} R_{\sigma\hat{s}\gamma\lambda}. \tag{17}$$

Here, $C^{[j]}_{\alpha\hat{s}\beta\hat{s}}$ and $\mathcal{C}_{\beta\sigma}(\hat{s}) = \mathcal{C}_{\beta\hat{s}\sigma\hat{s}}$ are the projections along $\hat{s}$ of the flexoelectric coupling [33] and elastic tensors, respectively. The second term in Eq. (17) originates from the relaxation of the acoustic modes, which produce a strain gradient (and hence atomic forces via flexoelectricity) at first order in q.

By combining the sum rule Eq. (14) with its flexoelectric counterpart [24,25], $\sum_j C^{[j]}_{\alpha\beta\gamma\lambda} = \mathcal{C}_{\alpha\beta\gamma\lambda}$, it is straightforward to verify that the sublattice sum of the renormalized force-response coefficients $|\tilde{K}_{\gamma\lambda}(\hat{s})\rangle$ identically vanishes. This guarantees [38] that the total polarization P_α is well defined, proving our point. Conversely, the individual contributions to P_α associated with the two terms in Eq. (17) depend on how the pseudoinverse is constructed [26], and are therefore ill defined as stand-alone properties. Such intimate relationship between the direct flexo-like contribution to the atomic forces [first term in Eq. (17)] and the "nonanalytic elastic contribution" of the second term provide a nice illustration of the covariance principle of Ref. [26], which we generalize here to the nonlinear regime. These conclusions have direct implications for the continuum modeling of inhomogeneous ferroelectric [20,39,40] and ferroelastic [5,21,22,41,42] structures, where the aforementioned two mechanisms play a central role. In particular, they clarify the relation between the "flexoantiferrodistortive" [5] and "flexoroto" [22] effects [corresponding to the first and second term in Eq. (17), respectively] described in the recent literature, and the necessity to account for both in order to obtain quantitatively accurate physical answers.

As a representative demonstration of the above arguments, we consider the case where the field $\boldsymbol{\phi}$ corresponds to the out-of-phase AFD tilts in perovskite-structure oxides, with $\mathrm{SrTiO_3}$ [21] as a test case. Calculations of the rotopolar [21] force-response tensor $|w_{\beta\gamma\lambda}\rangle$ (its symmetric part, $|K_{\beta\gamma\lambda}\rangle = (|w_{\beta\gamma\lambda}\rangle + |w_{\beta\lambda\gamma}\rangle)/4$, corresponds to the "flexo-AFD" effect described in Ref. [5]) are carried out within the framework of the local-density approximation (LDA) to density-functional theory as implemented in the ABINIT [31,43–45] package. We use a nonprimitive cell of 10 atoms in order to accommodate a small uniform tilt ϕ^0_α in the structure, which allows us to treat the third derivatives of Eq. (10) via finite differences in ϕ^0_α. The parametrization of the AFD mode amplitudes, in length units, follows the established convention [21,46]; relaxation of the antiferroelectric R mode of Ti [21,23] is fully accounted for in the calculated $W^{[i]}_{\alpha\beta\gamma\lambda}$ coefficients. Numerical results, details of the method and additional supporting data are reported in Ref. [33]; of particular note, we provide [33] a stringent numerical proof of the sum rule, Eq. (14), which we base on an independent calculation of the $\mathbf{R}$ (rotostriction [5,21,22]) tensor.

To illustrate the physical meaning of the calculated rotopolar coefficients, and as a further numerical validation thereof, we next consider a frozen-in cycloidal [21] tilt pattern in the form $\phi_s = \phi\cos(\mathbf{q}\cdot\mathbf{r})$, $\phi_r = \phi\sin(\mathbf{q}\cdot\mathbf{r})$, $\phi_z = 0$, where both the AFD pseudovector $\boldsymbol{\phi}$ and the propagation direction $\mathbf{q} = q\hat{s} = q[\cos(\theta), \sin(\theta), 0]$ lie in the pseudocubic xy plane. [Here, $\hat{r} = \hat{z}\times\hat{s}$ is the in-plane direction that is orthogonal to $\mathbf{q}$.] Our long-wavelength approach predicts, for the symmetry-adapted sublattice mode $[i]$, a *geometric* force (both DM- and flexo-type couplings are linear in P, which implies an improper [47–50] mechanism for local inversion-symmetry breaking) at a given point $\mathbf{r}$ in the crystal, whose transverse component reads as

$$f^{[i]}_r(\mathbf{r}) = \phi^2 q\left[\zeta^{[i]} + 2K^{[i]}(\hat{q})\cos(2\mathbf{q}\cdot\mathbf{r})\right]. \qquad (18)$$

($K^{[i]}(\hat{q}) = K^{[i]}_{rsrs}$ stand for the 1212 components of the flexo-type tensor in the rotated $\hat{s}, \hat{r}, \hat{z}$ system.) In Fig. 1(a) we compare the prediction of Eq. (18) with the forces that we obtain via a direct first-principles calculation of the AFD cycloid. (We use $\theta = \pi/4$, corresponding to $\hat{s}\|[110]$ in the pseudocubic system, and $q = 2\pi/(12\sqrt{2}a_0)$, which we accommodate in a 120-atom supercell; the tilt amplitude is set to $|\boldsymbol{\phi}| = 0.02a_0$, i.e., to a tilt angle of 2.3°.) The agreement is excellent, with a discrepancy of the order of a few percents at most. Note the qualitative difference between the uniform DM-like contribution to $f^{[i]}_r$ (dashed lines), and the spatially modulated flexo-like term, which averages to zero in any periodic tilt pattern.

The uniform DM-like forces sum up to zero, consistent with the translational symmetry of the crystal and with our

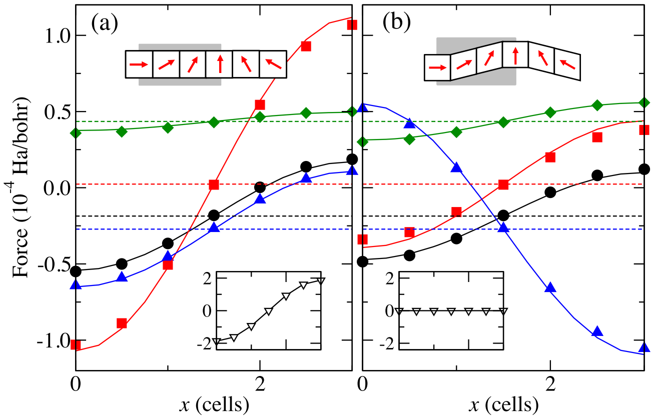

FIG. 1. Comparison between the atomic forces extracted from a direct calculation of an AFD cycloid (symbols) and the predictions of the macroscopic model (solid curves). Forces on Sr (black circles), Ti (red squares), and the "radial" (blue triangles) and "tangential" (green diamonds) oxygen modes of T_{1u} symmetry are shown. Dashed lines show the uniform DM-like forces. (a) No elastic relaxation; (b) mechanical equilibrium. Lower insets show the sublattice sum of the forces: first-principles (triangles) and model (solid curve). Upper insets schematically illustrate the portion (shaded gray area) of the fixed- or relaxed-strain cycloidal pattern shown in the main panel.

formal results. Conversely, the flexo-like forces display the expected drift, shown in the inset of Fig. 1(a), that originates from the strain coupling via Eq. (14). To verify that the net drift disappears at mechanical equilibrium, we determine the elastic displacement amplitude via $u(s) = -\phi^2 R_{rsrs}/(2qC_{rsrs})\cos(2qs)$. After incorporating $u(s)$ into the simulation cell, we recalculate the forces from first principles, and compare them in Fig. 1(b) with the predictions of Eq. (17). [The latter implies an additional contribution to Eq. (18) of the type $\Delta f_r^{[i]} = -4q^2 C_{rsrs}^{[i]} u(s)$.] Again, the agreement is excellent, and the elastic forces (inset) now vanish as expected. Note the drastic change in the amplitude of the forces on the Ti and radial-oxygen mode following elastic relaxation, while the Sr and tangential-oxygen modes are largely unaffected. This behavior stems from the fact that $C_{rsrs}^{[i]}$ is large and positive for $i = 2, 3$ and almost negligible otherwise (see Table S7 [33]).

The usefulness of the present theory is especially manifest in materials like $SrTiO_3$, where the lowest-frequency ("soft") mode at the zone center carries 99% of the polar response to a static perturbation. This observation leads to a compact representation of the physical effects described insofar as terms of a few materials-specific parameters; their calculated values are reported in Table S9 [33]. The information therein allows one to calculate the local polarization in an arbitrary inhomogeneous tilt structure via Eq. (16). For example, in the cycloid model of Fig. 1, which is representative of the typical inhomogeneities of the order parameter in the ferroelastic phase of $SrTiO_3$, we obtain a macroscopic polarization of $P = -0.9\ \mu C/cm^2$. The effect increases linearly with the static dielectric constant, ϵ, which should lead to values of P that are at least an order of magnitude larger at low temperature. ($\epsilon \simeq 900$ in our LDA calculations).

In summary, the trilinear Lifshitz invariants of Eqs. (1) and (2) emerge here as a rich and barely tapped playground of potentially useful crystal properties, thus opening many opportunities for future research. Examples of target applications range from the study of inhomogeneous structures in tilt-driven ferroelastics (e.g., $LaAlO_3$ or $CaTiO_3$) and antiferroelectrics [6], to testing the recent phenomenological prediction [19] of stable polar skyrmions in chiral systems. We shall explore these promising directions in the context of forthcoming publications.

We acknowledge support from Ministerio de Ciencia Y Innovación (MICINN-Spain) through Grant No. PID2019–108573 GB-C22; from Severo Ochoa FUNFUTURE center of excellence (CEX2019-000917-S); from Generalitat de Catalunya (Grant No. 2021 SGR 01519); and from the European Research Council (ERC) under the European Union's Horizon 2020 research and innovation program (Grant Agreement No. 724529).

*mstengel@icmab.es

[1] Albert Fert, Nicolas Reyren, and Vincent Cros, Magnetic skyrmions: Advances in physics and potential applications, Nat. Rev. Mater. **2**, 17031 (2017).
[2] Dennis Meier, Functional domain walls in multiferroics, J. Phys. Condens. Matter **27**, 463003 (2015).
[3] Piush Behera *et al.*, Electric field control of chirality, Sci. Adv. **8**, eabj8030 (2022).
[4] Ivan I. Naumov, L. Bellaiche, and Huaxiang Fu, Unusual phase transitions in ferroelectric nanodisks and nanorods, Nature (London) **432**, 737 (2004).
[5] Eugene A. Eliseev, Sergei V. Kalinin, Yijia Gu, Maya D. Glinchuk, Victoria Khist, Albina Borisevich, Venkatraman Gopalan, Long-Qing Chen, and Anna N. Morozovska, Universal emergence of spatially modulated structures induced by flexoantiferrodistortive coupling in multiferroics, Phys. Rev. B **88**, 224105 (2013).
[6] Konstantin Shapovalov and Massimiliano Stengel, Tilt-driven antiferroelectricity in $PbZrO_3$, Phys. Rev. Mater. **7**, L071401 (2023).
[7] Henning Pöttker and Ekhard K. H. Salje, Flexoelectricity, incommensurate phases and the Lifshitz point, J. Phys. Condens. Matter **28**, 075902 (2016).
[8] I. Dzyaloshinsky, A thermodynamic theory of weak ferromagnetism of antiferromagnetics, J. Phys. Chem. Solids **4**, 241 (1958).
[9] Tôru Moriya, Anisotropic superexchange interaction and weak ferromagnetism, Phys. Rev. **120**, 91 (1960).
[10] Maxim Mostovoy, Ferroelectricity in spiral magnets, Phys. Rev. Lett. **96**, 067601 (2006).
[11] A. Sparavigna, A. Strigazzi, and A. Zvezdin, Electric-field effects on the spin-density wave in magnetic ferroelectrics, Phys. Rev. B **50**, 2953 (1994).
[12] Amelia Sparavigna, Role of Lifshitz invariants in liquid crystals, Materials **2**, 674 (2009).
[13] Di Xiao, Junren Shi, Dennis P. Clougherty, and Qian Niu, Polarization and adiabatic pumping in inhomogeneous crystals, Phys. Rev. Lett. **102**, 087602 (2009).
[14] P. Zubko, G. Catalan, and A. K. Tagantsev, Flexoelectric effect in solids, Annu. Rev. Mater. Res. **43**, 387 (2013).
[15] Massimiliano Stengel and David Vanderbilt, First-principles theory of flexoelectricity, in *Flexoelectricity in Solids from Theory to Applications*, edited by Alexander K. Tagantsev and Petr V. Yudin (World Scientific Publishing Co., Singapore, 2016), Chap. 2, pp. 31–110.
[16] A. L. Korzhenevskii, On the theory of phase transitions into inhomogeneous states, Sov. Phys. JETP **54**, 568 (1981), http://www.jetp.ras.ru/cgi-bin/e/index/e/54/3/p568?a=list.
[17] A. P. Pyatakov, A. S. Sergeev, F. A. Mikailzade, and A. K. Zvezdin, Spin flexoelectricity and chiral spin structures in magnetic films, J. Magn. Magn. Mater. **383**, 255 (2015), selected papers from the sixth Moscow International Symposium on Magnetism (MISM-2014).
[18] Hong Jian Zhao, Peng Chen, Sergey Prosandeev, Sergey Artyukhin, and Laurent Bellaiche, Dzyaloshinskii-Moriya–like interaction in ferroelectrics and antiferroelectrics, Nat. Mater. **20**, 341 (2021).
[19] K. C. Erb and J. Hlinka, Vector, bidirector, and Bloch skyrmion phases induced by structural crystallographic symmetry breaking, Phys. Rev. B **102**, 024110 (2020).

[20] Peng Chen, Hong Jian Zhao, Sergey Prosandeev, Sergey Artyukhin, and Laurent Bellaiche, Microscopic origin of the electric Dzyaloshinskii-Moriya interaction, Phys. Rev. B **106**, 224101 (2022).

[21] Andrea Schiaffino and Massimiliano Stengel, Macroscopic polarization from antiferrodistortive cycloids in ferroelastic $SrTiO_3$, Phys. Rev. Lett. **119**, 137601 (2017).

[22] Anna N. Morozovska, Eugene A. Eliseev, Maya D. Glinchuk, Long-Qing Chen, and Venkatraman Gopalan, Interfacial polarization and pyroelectricity in antiferrodistortive structures induced by a flexoelectric effect and rotostriction, Phys. Rev. B **85**, 094107 (2012).

[23] Blai Casals, Andrea Schiaffino, Arianna Casiraghi, Sampo J. Hämäläinen, Diego López González, Sebastiaan van Dijken, Massimiliano Stengel, and Gervasi Herranz, Low-temperature dielectric anisotropy driven by an antiferroelectric mode in $SrTiO_3$, Phys. Rev. Lett. **120**, 217601 (2018).

[24] M. Stengel, Flexoelectricity from density-functional perturbation theory, Phys. Rev. B **88**, 174106 (2013).

[25] Miquel Royo and Massimiliano Stengel, Lattice-mediated bulk flexoelectricity from first principles, Phys. Rev. B **105**, 064101 (2022).

[26] Oswaldo Diéguez and Massimiliano Stengel, Translational covariance of flexoelectricity at ferroelectric domain walls, Phys. Rev. X **12**, 031002 (2022).

[27] Miquel Royo and Massimiliano Stengel, First-principles theory of spatial dispersion: Dynamical quadrupoles and flexoelectricity, Phys. Rev. X **9**, 021050 (2019).

[28] S. Baroni, S. de Gironcoli, and A. Dal Corso, Phonons and related crystal properties from density-functional perturbation theory, Rev. Mod. Phys. **73**, 515 (2001).

[29] X. Gonze and C. Lee, Dynamical matrices, Born effective charges, dielectric permittivity tensors, and interatomic force constants from density-functional perturbation theory, Phys. Rev. B **55**, 10355 (1997).

[30] X. Gonze *et al.*, ABINIT: First-principles approach to material and nanosystem properties, Comput. Phys. Commun. **180**, 2582 (2009).

[31] Aldo H. Romero *et al.*, ABINIT: Overview and focus on selected capabilities, J. Chem. Phys. **152**, 124102 (2020).

[32] ABINIT is an open-source code, distributed under the GNU General Public Licence. All material (postprocessing scripts, input files) developed in this work is available upon request, and will be incorporated in future public releases.

[33] See Supplemental Material at http://link.aps.org/supplemental/10.1103/PhysRevLett.132.146801 for a description of the notation, supporting analytical derivations and numerical results.

[34] J. Hong and D. Vanderbilt, First-principles theory and calculation of flexoelectricity, Phys. Rev. B **88**, 174107 (2013).

[35] R. Resta, L. Colombo, and S. Baroni, Absolute deformation potentials in semiconductors, Phys. Rev. B **41**, 12358 (1990).

[36] Massimiliano Stengel, Unified *ab initio* formulation of flexoelectricity and strain-gradient elasticity, Phys. Rev. B **93**, 245107 (2016).

[37] Kevin F. Garrity, Karin M. Rabe, and David Vanderbilt, Hyperferroelectrics: Proper ferroelectrics with persistent polarization, Phys. Rev. Lett. **112**, 127601 (2014).

[38] Max Born and Kun Huang, *Dynamical Theory of Crystal Lattices* (Oxford University Press, Oxford, 1954).

[39] P. V. Yudin, A. K. Tagantsev, E. A. Eliseev, A. N. Morozovska, and N. Setter, Bichiral structure of ferroelectric domain walls driven by flexoelectricity, Phys. Rev. B **86**, 134102 (2012).

[40] Yijia Gu, Menglei Li, Anna N. Morozovska, Yi Wang, Eugene A. Eliseev, Venkatraman Gopalan, and Long-Qing Chen, Flexoelectricity and ferroelectric domain wall structures: Phase-field modeling and DFT calculations, Phys. Rev. B **89**, 174111 (2014).

[41] W. Schranz, C. Schuster, A. Tröster, and I. Rychetsky, Polarization of domain boundaries in $SrTiO_3$ studied by layer group and order-parameter symmetry, Phys. Rev. B **102**, 184101 (2020).

[42] A. Tröster, C. Verdi, C. Dellago, I. Rychetsky, G. Kresse, and W. Schranz, Hard antiphase domain boundaries in strontium titanate unravelled using machine-learned force fields, Phys. Rev. Mater. **6**, 094408 (2022).

[43] X. Gonze *et al.*, Recent developments in the ABINIT software package, Comput. Phys. Commun. **205**, 106 (2016).

[44] D. R. Hamann, Optimized norm-conserving Vanderbilt pseudopotentials, Phys. Rev. B **88**, 085117 (2013).

[45] M. J. van Setten, M. Giantomassi, E. Bousquet, M. J. Verstraete, D. R. Hamann, X. Gonze, and G.-M. Rignanese, The PseudoDojo: Training and grading a 85 element optimized norm-conserving pseudopotential table, Comput. Phys. Commun. **226**, 39 (2018).

[46] Wenwu Cao and Gerhard R. Barsch, Landau-Ginzburg model of interphase boundaries in improper ferroelastic Perovskites of D_{4h}^{18} symmetry, Phys. Rev. B **41**, 4334 (1990).

[47] Massimiliano Stengel, Craig J. Fennie, and Philippe Ghosez, Electrical properties of improper ferroelectrics from first principles, Phys. Rev. B **86**, 094112 (2012).

[48] Eric Bousquet, Matthew Dawber, Nicolas Stucki, C. Lichtensteiger, Patrick Hermet, Stefano Gariglio, Jean-Marc Triscone, and Philippe Ghosez, Improper ferroelectricity in perovskite oxide artificial superlattices, Nature (London) **452**, 732 (2008).

[49] Craig J. Fennie and Karin M. Rabe, Ferroelectric transition in $YMnO_3$ from first principles, Phys. Rev. B **72**, 100103(R) (2005).

[50] Nicole A. Benedek and Craig J. Fennie, Hybrid improper ferroelectricity: A mechanism for controllable polarization-magnetization coupling, Phys. Rev. Lett. **106**, 107204 (2011).